



# Plant-based triboelectric nanogenerator for biomechanical energy harvesting

Anjaly Babu<sup>a</sup>, D. Rakesh<sup>b</sup>, P. Supraja<sup>a</sup>, Siju Mishra<sup>a</sup>, K. Uday Kumar<sup>a,\*</sup>, R. Rakesh Kumar<sup>a,\*</sup>, D. Haranath<sup>a</sup>, Estari Mamidala<sup>b</sup>, Raju Nagapuri<sup>c</sup>

<sup>a</sup> Department of Physics, Energy Materials and Devices Lab, National Institute of Technology, Warangal, 506004, India

<sup>b</sup> Infectious Diseases Research Lab, Department of Zoology, Kakatiya University, Warangal 506009, India

<sup>c</sup> Department of Physics, Osmania University, Hyderabad, 500007, India

## ARTICLE INFO

### Keywords:

Green energy  
Energy harvesting  
Triboelectric nanogenerator  
Vertical contact separation mode  
R. vesicarius plant leaves

## ABSTRACT

As people became more aware of environmental issues, several designs of triboelectric energy harvesters based on biocompatible and eco-friendly natural materials have been developed in recent years. This manuscript reports a plant-based green triboelectric nanogenerator using extracted leaf powder of the *Rumex vesicarius* plant and PET as triboelectric layers. When hand-tapped, the developed TENG generated an open-circuit voltage ( $V_{oc}$ ) of 3.86 V, and a short-circuit current ( $I_{sc}$ ) of 3.78  $\mu$ A, respectively. The device has the highest power density of 0.1894  $\mu$ W/cm<sup>2</sup> at load resistances of  $\sim$ 20 M $\Omega$  and can directly power up one light-emitting diode. The TENG response has been tested over 1200 cycles, confirming its remarkable stability. The proposed TENG can be a promising sustainable tool to capture mechanical energy from nature and our everyday actions and thus convert it into electricity.

## 1. Introduction

Over the decades, harvesting energy from the living environment has been a global area of research due to its potential to produce clean and sustainable energy to combat the energy crisis and the growing environmental issues caused by fossil fuels (Silva, 2013). Energy harvesting technologies have been developed to transform renewable energy sources such as solar, wave, tidal, and wind into electrical energy to power a wide range of devices from micro to large-scale systems (Dambhare et al., 2021; Wang et al., 2018; Zheng et al., 2022). However, these energy resources require ample installation space and maintenance costs, are confined to specific locations, are larger, and depend on weather conditions.

Unlike other renewable energy sources, mechanical energy is safe, available everywhere, and considered the most promising candidate to meet increasing energy requirements. Various methods have been proposed to extract electricity from mechanical energy such as human motion, wind, water waves, or other kinds of mechanical vibration based on triboelectric, piezoelectric, and electromagnetic mechanisms (Zhou et al., 2018; Zheng et al., 2017; Hu and Wang, 2014; Wang and Chang, 2010). Triboelectric energy harvesting exhibits high energy conversion efficiency, high output power, simple structure, flexibility, low production cost, and a broad selection of materials (Luo and Wang, 2020; Zhu et al., 2020; Walden et al., 2022; Li et al., 2020; Yang et al., 2022a; Luo et al., 2022; Hu et al., 2022; Zhang et al., 2021). Prof. Z.L Wang coined triboelectric generator/ triboelectric nanogenerator names for

triboelectric energy harvesting device (Wang and Song, 2006; Xu et al., 2010). Triboelectric nanogenerators (TENGs) have recently emerged as a very powerful method for harvesting mechanical energy into electrical energy based on the triboelectric effect and electrostatic induction. TENG's vertical contact-separation (VCS) mode is best because of its simple structure design, and physical damage due to the frictional force between tribolayers is less than others (Supraja et al., 2022; Hasan et al., 2022). The triboelectric layer material is the core element of the TENG, which determines its output performance; therefore, exploration and use of novel materials are critical areas of TENG research (Zhang and Olin, 2020; Kim et al., 2020). In this manuscript, we used the vertical contact-separation mode of TENG.

The most commonly used friction layers are polytetrafluoroethylene (PTFE), fluorinated ethylene propylene (FEP), polyethylene terephthalate (PET), PDMS, PVDF, Nylon, Kapton, Cu, Al, ITO, Graphene, few are expensive and non-biodegradable (Dzhardimalieva et al., 2021; Ko et al., 2014; Nurmakanov et al., 2021). As people become increasingly concerned about environmental protection, it is crucial to identify a triboelectric material with excellent biocompatibility, degradability, and triboelectric effect. Researchers have recently opened up the possibility of using natural materials such as leaves (Jie et al., 2018; Feng et al., 2019), wood (Luo et al., 2019; Hao et al., 2020), flowers (Chen et al., 2018), egg white, chitin (Jiang et al., 2018), spider web (Zhang et al., 2018), rice paper (Chi et al., 2019; Slabov et al., 2020). In this study, we demonstrated for the first-time leaves powder from *Rumex vesicarius*

\* Corresponding authors.

E-mail addresses: [kanapuram.udaykumar@nitw.ac.in](mailto:kanapuram.udaykumar@nitw.ac.in) (K.U. Kumar), [rakeshr@nitw.ac.in](mailto:rakeshr@nitw.ac.in) (R.R. Kumar).

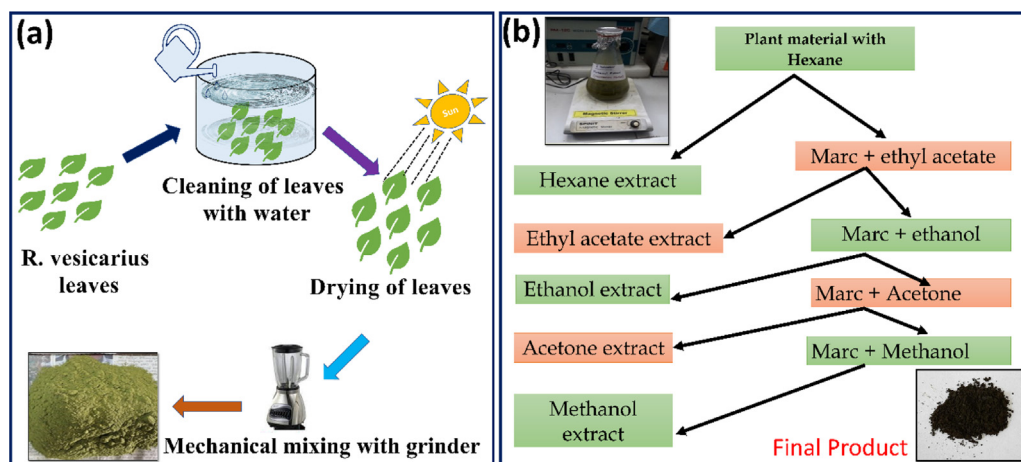


Fig. 1. (a) Schematic of the *R. vesicarius* leaves powder preparation and obtained powder (e) Flow chart showing the sequential maceration method (lower inset shows the synthesized leaves powder).

(*R. vesicarius*) plants as natural candidate for the development of triboelectric nanogenerators. The triboelectric nanogenerator was fabricated using dried *R. vesicarius* leaves powder and PET as the triboelectric layers in VCS mode to harvest mechanical energy. It is reported in the literature that leaves powder-based TENG exhibits high output power compared to leaves-based TENG (Feng et al., 2019). Therefore, we preferred to use *R. vesicarius* leaves powder instead of direct leaves in the present work.

## 2. Experimental method

### 2.1. Materials

ITO-PET substrates with sheet resistance ( $60 \Omega/\square$ ) were obtained from Sigma Aldrich, aluminum (Al) foil of 0.1 mm thickness purchased from Special metals Pvt. Ltd. Cardboards, sponges, LEDs were brought from a local market.

### 2.2. Preparation of leaves powder and its film on aluminum substrate

Fig. 1(a) shows the schematic of the different stages of leaves powder preparation. The leaves of *R. vesicarius* were collected in bulk from the local area of Warangal, Telangana state, India (Davella and Mamidala, 2021). The collected leaves were washed and dried in the shade at room temperature until they were free from dust and moisture. Using a mechanical mixer, the dried leaves were then reduced to a coarse powder. Sequential maceration process using non-polar to polar solvents (hexane, ethyl acetate, acetone, and methanol) was used to get powder extract, as shown in the flow chart in Fig. 1(b). The bottom inset of Fig. 1(b) shows the final extracted leaves powder. The extracted leaves powder was dispensed in a solution mixture of ethanol and deionized water (1:1 ratio) and kept under sonication for 20 min to get the uniform solution, as shown in Fig. 2(a). The resulting solution was drop cast onto a clean aluminum foil ( $6 \times 6 \text{ cm}^2$ ) and dried at  $40^\circ \text{C}$  for 1 h. Fig. 2(c) shows the deposited film on the aluminum foil.

### 2.3. Fabrication of TENG device

Fig. 2(b) shows a schematic of the TENG device in VCS mode and its components. Initially, leaves powder-coated aluminum foil and ITO-PET were attached to the cardboard base, as shown in Fig. 2(c)–(d). Aluminum foil and ITO surface serve as electrodes for the TENG device ( $5 \times 5 \text{ cm}^2$ ). Finally, both geometries were connected using a sponge spacer and attached to connecting wires, as shown in Fig. 2(e). Bio-mechanical (hand slapping) force was repeatedly applied to the TENG device and recorded its electrical output response. The TENG voltage and current were recorded using a digital oscilloscope (Tektronix TBS1102) and a low-noise current preamplifier (SRS, SR 570).

## 3. Results and discussion

The surface of the prepared *R. vesicarius* leaves powder film was examined using SEM, and the corresponding images at different magnifications are shown in Fig. 3(a)–(c). It is clear from the SEM images that the prepared film has microlevel roughness. This high roughness of *R. vesicarius* leaves powder film makes fewer contact points with PET during the TENG operation, significantly affecting TENG performance. Further, energy dispersive X-ray (EDX) analysis was performed, and the corresponding spectrum is shown in Fig. 3(d). EDX spectrum reveals the presence of O, Na, Si, Mg, P, Cl, K, and Ca. The weight percentage of different elements are shown in the inset of Fig. 3(d).

Fig. 4(a) – (b) shows the open-circuit voltage ( $V_{oc}$ ) and short circuit current ( $I_{sc}$ ) of the fabricated TENG in forward and reverse connections, respectively. The  $V_{oc}$  and  $I_{sc}$  of  $\sim 3.86 \text{ V}$  and  $\sim 3.78 \mu\text{A}$  were observed for the TENG device for repeated hand tapping. A switching polarity test was performed by reversing the TENG input connection to the oscilloscope to confirm that the output response is only due to the fabricated TENG. The polarity test shows that the output voltage/current is the same in both connections geometry and thus confirms the voltage/current is generated from the developed TENG and not from the instrument noise. The low output voltage for the TENG can be explained using high roughness observed in the SEM images of leaf powder film. This high roughness produces only a few contact points with PET during TENG operation, which results in low output.

Fig. 4(e) depicts the working mechanism of the fabricated leaf-TENG based on the coupling effect of triboelectrification and electrostatic induction. In the original state, leaves powder film and PET friction layers are separated and in an electrically neutral state; therefore, no electricity is produced. When a mechanical force is applied, the PET layer is brought into contact with leaves powder film in VSC mode.

Due to the difference in electron affinity between the materials, positive and negative charges are developed on the surface of PET and leaves powder film, respectively. When the triboelectric layers separate, resulting in a potential difference between the electrodes. The induced potential difference drives the electrons from ITO to Al electrodes through an external load that produces an output current. Current flow continues until the charges reach a state of equilibrium. When the triboelectric layers are brought back into contact, a reversed output current is generated in the circuit. An alternating current is created in the external circuit with periodic contact and separation of the tribolayers through mechanical force.

The  $V_{oc}$  and  $I_{sc}$  of fabricated TENG were measured at different load resistances ( $10 \text{ K}\Omega$  –  $100 \text{ M}\Omega$ ) to determine the maximum output power density. The variation of the output voltage and current with

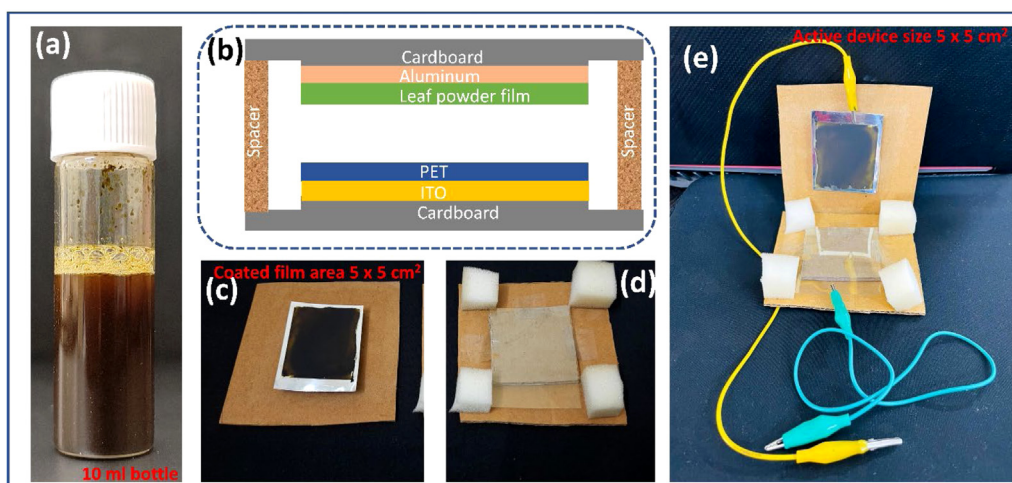


Fig. 2. (a) Solution of extracted leaves powder, (b) Schematic diagram of the fabricated TENG device, (c) leaves powder film on aluminum foil and its attachment to cardboard sheet, (d) ITO/PET substrate attached to another cardboard sheet with PET side facing up, (e) final fabricated TENG device with top layer as leaves powder film/Al substrate and bottom layer as ITO/PET and its electrode connections.

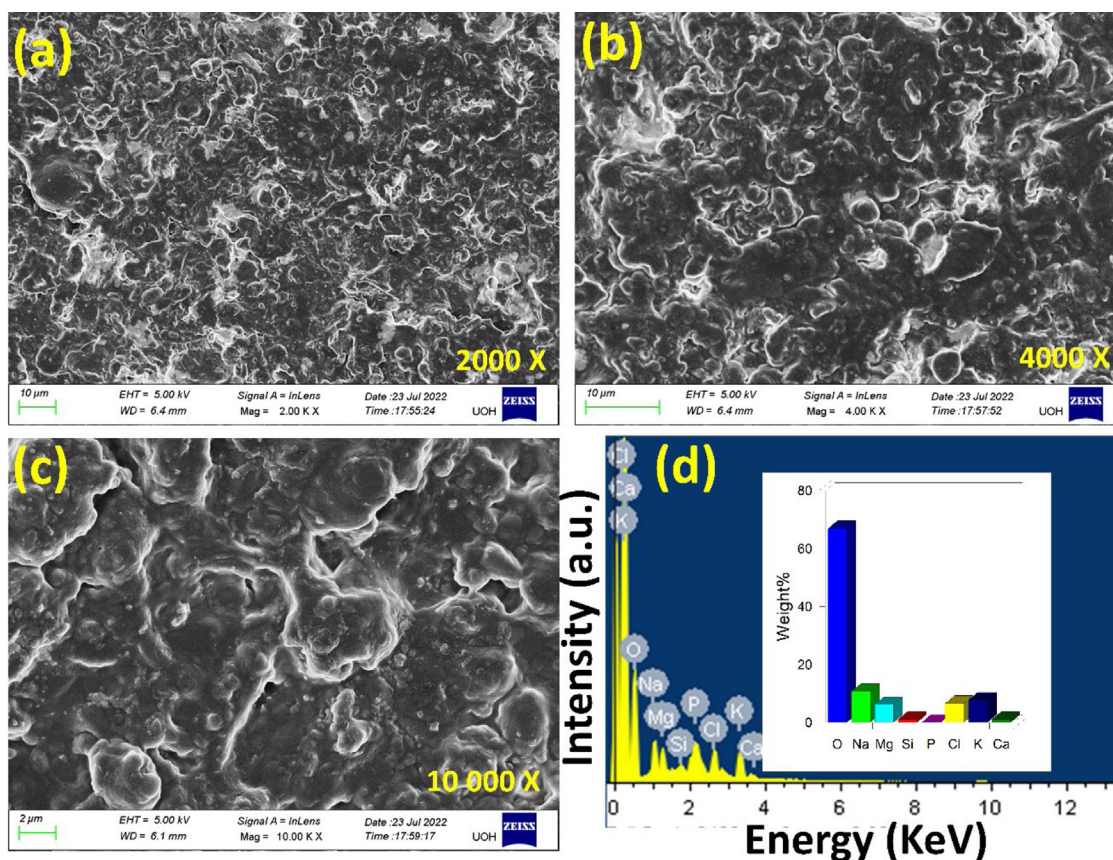


Fig. 3. (a)–(c) Surface of the *R. vesicarius* leaves powder film SEM images at different magnifications, (d) EDX spectrum of *R. vesicarius* leaves powder film (inset weight percentage of elements).

the resistance is shown in Fig. 4(c). The output voltage increases with the load resistance and saturates at a higher resistance value from 37.69 M $\Omega$ . Due to ohmic losses, the current starts at 3.72  $\mu$ A at 200 K $\Omega$  and decreases with the load resistance (Niu et al., 2015). The instantaneous power of TENG was calculated from the equation  $P = IV$ , and the highest output power, 4.75  $\mu$ W, was obtained at a load resistance  $\sim$ 20 M $\Omega$  (see supplementary information SI, S1) (Bird, 2003). The instantaneous power density was calculated by considering the active area of the device and found  $\sim$ 0.1894  $\mu$ W/cm<sup>2</sup> at a load

resistance of  $\sim$ 20 M $\Omega$ , as shown in Fig. 4(d). The highest power density at 20 M $\Omega$  is due to impedance matching conditions (Bird, 2003). The TENG's low output power can be improved by selecting the second triboelectric layer such as PDMS, FEP, and PTFE instead of PET (Yang et al., 2022b). In another strategy, leaf powder can be ball milled to get the film with nanoscale roughness. The nanoscale roughness creates more contact points with PET during TENG operation, effectively improving the TENG output. In addition, surface modification which includes physical modification (Zhao et al., 2016), chemical

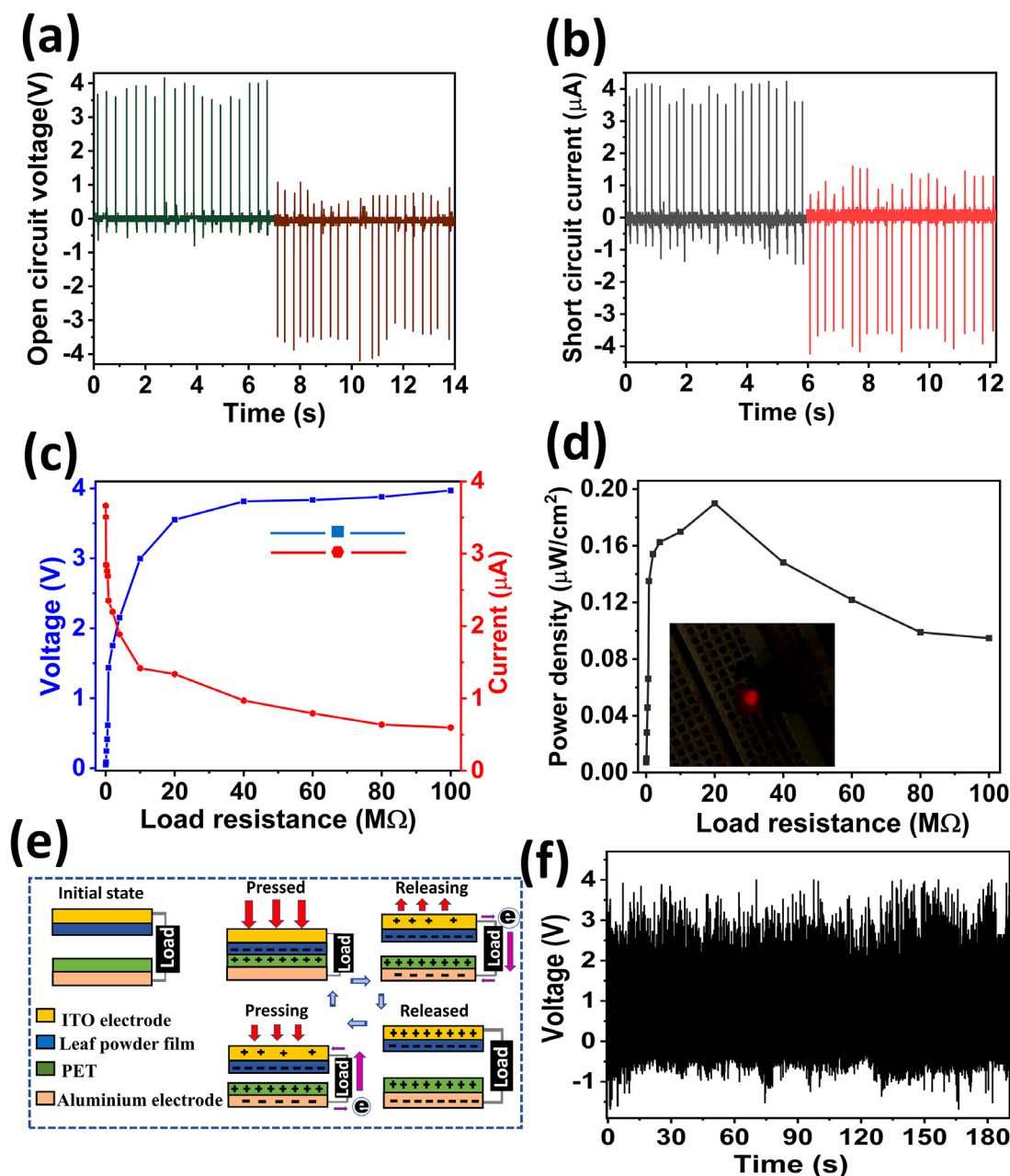


Fig. 4. (a)  $V_{oc}$  of TENG device under switching polarity test, (b)  $I_{sc}$  of TENG device under switching polarity test, (c)  $V_{oc}$  and  $I_{sc}$  measured as a function of different load resistances, (d) instantaneous power density of the TENG device as a function of load resistance, (e) schematic illustration of the working mechanism of TENG in vertical contact-separation mode, (f) TENG stability test under 1200 cycles.

surface functionalization (Lin et al., 2013), surface ion injection (Wang et al., 2014) and use of liquid-dielectric/electrode (Li et al., 2018) are also considered best for TENG output improvement. In addition to the above, standardization of TENG and finite element simulations of TENG will provide new insights in improving the TENG performance (Li et al., 2019b,a). Further, the fabricated TENG can turn on one LED directly without using any charged capacitor. The snapshot of the glowing LED powered by TENG is shown in the inset of Fig. 4(d) (See **supplementary video V1**). The applications of TENG can be further extended to self-powered humidity sensors (Su et al., 2017), touch sensors (Jeong et al., 2020), health monitoring (Cao et al., 2018).

Finally, to examine the stability and durability, the output voltage of the fabricated TENG was tested over 1200 cycles, and the responses are shown in Fig. 4(f). The generated output voltage did not vary considerably; hence the fabricated device exhibits high stability. The

minor deviation in the output voltage is due to the variation in hand tapping.

#### 4. Conclusion

In this work, a TENG based on biodegradable leaves powder of *R. vesicarius* was fabricated for the first instance to harvest the mechanical energy from the surrounding. The measured open-circuit voltage and short circuit current of the fabricated TENG are 3.86 V and 3.78  $\mu$ A, respectively. The TENG device with an area of 25 cm<sup>2</sup> shows a power density of 0.1894  $\mu$ W/cm<sup>2</sup> at load resistances of 20 M $\Omega$ . As a power source, it can light up one light-emitting diode directly. A stability test of TENG was performed for 1200 cycles, and the output voltages were found to be essentially invariant. The leaf powder-based TENG, which is inexpensive and biodegradable, is ideal for mechanical energy harvesting and green energy sources.

## Declaration of competing interest

The authors declare that they have no known competing financial interests or personal relationships that could have appeared to influence the work reported in this paper.

## Acknowledgments

The authors would like to thank the Department of Physics and Centre for Research and Instrument facility (CRIF), NIT-Warangal, for providing their research facilities.

## Appendix A. Supplementary data

Supplementary material related to this article can be found online at <https://doi.org/10.1016/j.rsurfi.2022.100075>.

## References

- Bird, J., 2003. Electrical Circuit Theory and Technology. <http://dx.doi.org/10.4324/9780080505169>.
- Cao, R., Wang, J., Zhao, S., Yang, W., Yuan, Z., Yin, Y., Du, X., Li, N.W., Zhang, X., Li, X., Wang, Z.L., Li, C., 2018. Self-powered nanofiber-based screen-print triboelectric sensors for respiratory monitoring. *Nano Res.* 2017 7 (11), 3771–3779. <http://dx.doi.org/10.1007/S12274-017-1951-2>.
- Chen, Y., Jie, Y., Wang, J., Ma, J., Jia, X., Dou, W., Cao, X., 2018. Triboelectrification on natural rose petal for harvesting environmental mechanical energy. *Nano Energy* 50, 441–447. <http://dx.doi.org/10.1016/j.nanoen.2018.05.021>.
- Chi, Y., Xia, K., Zhu, Z., Fu, J., Zhang, H., Du, C., Xu, Z., 2019. Rice paper-based biodegradable triboelectric nanogenerator. *Microelectron. Eng.* 216, 111059. <http://dx.doi.org/10.1016/j.mee.2019.111059>.
- Dambhare, M.V., Butey, B., Moharil, S.V., 2021. Solar photovoltaic technology: A review of different types of solar cells and its future trends. *J. Phys. Conf. Ser.* 1913, <http://dx.doi.org/10.1088/1742-6596/1913/1/012053>.
- Davella, R., Mamidala, E., 2021. Luteolin: A potential multiple targeted drug effectively inhibits diabetes mellitus protein targets. *J. Pharm. Res. Int.* 161–171. <http://dx.doi.org/10.9734/jpri/2021/v33i44b32661>.
- Dzhardimalieva, G.I., Yadav, B.C., Lifintseva, T.V., Uflyand, I.E., 2021. Polymer chemistry underpinning materials for triboelectric nanogenerators (TENGs): Recent trends. *Eur. Polym. J.* 142, 110163. <http://dx.doi.org/10.1016/j.eurpolymj.2020.110163>.
- Feng, Y., Zhang, L., Zheng, Y., Wang, D., Zhou, F., Liu, W., 2019. Leaves based triboelectric nanogenerator (TENG) and TENG tree for wind energy harvesting. *Nano Energy* 55, 260–268. <http://dx.doi.org/10.1016/j.nanoen.2018.10.075>.
- Hao, S., Jiao, J., Chen, Y., Wang, Z.L., Cao, X., 2020. Natural wood-based triboelectric nanogenerator as self-powered sensing for smart homes and floors. *Nano Energy* 75, 104957. <http://dx.doi.org/10.1016/j.nanoen.2020.104957>.
- Hasan, S., Kouzani, A.Z., Adams, S., Long, J., Mahmud, M.A.P., 2022. Comparative study on the contact-separation mode triboelectric nanogenerator. *J. Electrostat.* 116, <http://dx.doi.org/10.1016/j.elstat.2022.103685>.
- Hu, S., Han, J., Shi, Z., Chen, K., Xu, N., Wang, Y., Zheng, R., Tao, Y., Sun, Q., Wang, Z.L., Yang, G., 2022. Biodegradable, super-strong, and conductive cellulose macrofibers for fabric-based triboelectric nanogenerator. *Nano-Micro Lett.* 14, 1–20. <http://dx.doi.org/10.1007/S40820-022-00858-W/FIGURES/6>.
- Hu, Y., Wang, Z.L., 2014. Recent progress in piezoelectric nanogenerators as a sustainable power source in self-powered systems and active sensors. *Nano Energy* 14, 3–14. <http://dx.doi.org/10.1016/j.nanoen.2014.11.038>.
- Jeong, J.B., Kim, H., il Yoo, J., 2020. Triboelectric touch sensor for position mapping during total hip arthroplasty. *BMC Res. Not.* 13, 1–5. <http://dx.doi.org/10.1186/S13104-020-05238-4/FIGURES/2>.
- Jiang, W., Li, H., Liu, Z., Li, Z., Tian, J., Shi, B., Zou, Y., Ouyang, H., Zhao, C., Zhao, L., Sun, R., Zheng, H., Fan, Y., Wang, Z.L., Li, Z., 2018. Fully bioabsorbable natural-materials-based triboelectric nanogenerators. *Adv. Mater.* 30, 1–10. <http://dx.doi.org/10.1002/adma.201801895>.
- Jie, Y., Jia, X., Zou, J., Chen, Y., Wang, N., Wang, Z.L., Cao, X., 2018. Natural leaf made triboelectric nanogenerator for harvesting environmental mechanical energy. *Adv. Energy Mater.* 8, 1–7. <http://dx.doi.org/10.1002/aenm.201703133>.
- Kim, D.W., Lee, J.H., Kim, J.K., Jeong, U., 2020. Material aspects of triboelectric energy generation and sensors. *NPG Asia Mater.* 12, <http://dx.doi.org/10.1038/s41427-019-0176-0>.
- Ko, Y.H., Nagaraju, G., Lee, S.H., Yu, J.S., 2014. PDMS-based triboelectric and transparent nanogenerators with ZnO nanorod arrays. *ACS Appl. Mater. Interfaces* 6 (9), 6631–6637. <http://dx.doi.org/10.1021/am5018072>.
- Li, X., Lau, T.H., Guan, D., Zi, Y., 2019a. A universal method for quantitative analysis of triboelectric nanogenerators. *J. Mat. Chem. A* 7, 19485–19494. <http://dx.doi.org/10.1039/C9TA06525C>.
- Li, X., Tao, J., Wang, X., Zhu, J., Pan, C., Wang, Z.L., 2018. Networks of high performance triboelectric nanogenerators based on liquid–solid interface contact electrification for harvesting low-frequency blue energy. *Adv. Energy Mater.* 8, 1800705. <http://dx.doi.org/10.1002/AENM.201800705>.
- Li, J., Wu, C., Dharmasena, I., Ni, X., Wang, Z., Shen, H., Huang, S.-L., Ding, W., 2020. Triboelectric nanogenerators enabled internet of things: A survey. *Intell. Converged Netw.* 1, 115–141. <http://dx.doi.org/10.23919/icn.2020.0008>.
- Li, X., Xu, G., Xia, X., Fu, J., Huang, L., Zi, Y., 2019b. Standardization of triboelectric nanogenerators: Progress and perspectives. *Nano Energy* 56, 40–55. <http://dx.doi.org/10.1016/j.nanoen.2018.11.029>.
- Lin, Z.H., Xie, Y., Yang, Y., Wang, S., Zhu, G., Wang, Z.L., 2013. Enhanced triboelectric nanogenerators and triboelectric nanosensor using chemically modified TiO<sub>2</sub> nanomaterials. *ACS Nano* 7, 4554–4560. [http://dx.doi.org/10.1021/NN401256W/SUPPL\\_FILE/NN401256W\\_SI\\_001.PDF](http://dx.doi.org/10.1021/NN401256W/SUPPL_FILE/NN401256W_SI_001.PDF).
- Luo, L., Han, J., Xiong, Y., Huo, Z., Dan, X., Yu, J., Yang, J., Li, L., Sun, J., Xie, X., Wang, Z.L., Sun, Q., 2022. Kirigami interactive triboelectric mechanologic. *Nano Energy* 99, 107345. <http://dx.doi.org/10.1016/J.NANOEN.2022.107345>.
- Luo, J., Wang, Z.L., 2020. Recent progress of triboelectric nanogenerators: From fundamental theory to practical applications. *EcoMat.* 2, 1–22. <http://dx.doi.org/10.1002/eom2.12059>.
- Luo, J., Wang, Z., Xu, L., Wang, A.C., Han, K., Jiang, T., Lai, Q., Bai, Y., Tang, W., Fan, F.R., Wang, Z.L., 2019. Flexible and durable wood-based triboelectric nanogenerators for self-powered sensing in athletic big data analytics. *Nature Commun.* 10, 1–9. <http://dx.doi.org/10.1038/s41467-019-13166-6>.
- Niu, S., Liu, Y., Zhou, Y.S., Wang, S., Lin, L., Wang, Z.L., 2015. Optimization of triboelectric nanogenerator charging systems for efficient energy harvesting and storage. *IEEE Trans. Electron Devices* 62, 641–647. <http://dx.doi.org/10.1109/TED.2014.2377728>.
- Nurmakanov, Y., Kalimuldina, G., Nauryzbayev, G., Adair, D., Bakenov, Z., 2021. Structural and chemical modifications towards high-performance of triboelectric nanogenerators. *Nanoscale Res. Lett.* 16, <http://dx.doi.org/10.1186/s11671-021-03578-z>.
- Silva, E., 2013. Environment and sustainable development. In: *Routledge Handbook of Latin American Politics*. pp. 181–199. <http://dx.doi.org/10.4324/9780203860267-22>.
- Slabov, V., Kopyl, S., Soares dos Santos, M.P., Kholkin, A.L., 2020. Natural and eco-friendly materials for triboelectric energy harvesting. *Nano-Micro Lett.* 12, <http://dx.doi.org/10.1007/s40820-020-0373-y>.
- Su, Y., Xie, G., Wang, S., Tai, H., Zhang, Q., Du, H., Du, X., Jiang, Y., 2017. Self-powered humidity sensor based on triboelectric nanogenerator. In: *Proceedings of IEEE Sensors 2017-December*. pp. 1–3. <http://dx.doi.org/10.1109/ICSENS.2017.8234280>.
- Supraja, P., Kumar, R.R., Mishra, S., Haranath, D., Sankar, R.R., Prakash, K., Jayarambabu, N., Rao, T.V., Kumar, K.U., 2022. A simple and low-cost triboelectric nanogenerator based on two dimensional ZnO nanosheets and its application in portable electronics. *Sensors Actuators A* 335, 113368. <http://dx.doi.org/10.1016/j.sna.2022.113368>.
- Walden, R., Kumar, C., Mulvihill, D.M., Pillai, S.C., 2022. Opportunities and challenges in triboelectric nanogenerator (TENG) based sustainable energy generation technologies: A mini-review. *Chem. Eng. J. Adv.* 9, 100237. <http://dx.doi.org/10.1016/j.cej.2021.100237>.
- Wang, D.A., Chang, K.H., 2010. Electromagnetic energy harvesting from flow induced vibration. *Microelectron. J.* 41, 356–364. <http://dx.doi.org/10.1016/j.mejo.2010.04.005>.
- Wang, H., Jasim, A., Chen, X., 2018. Energy harvesting technologies in roadway and bridge for different applications – A comprehensive review. *Appl. Energy* 212, 1083–1094. <http://dx.doi.org/10.1016/j.apenergy.2017.12.125>.
- Wang, Z.L., Song, J., 2006. Piezoelectric nanogenerators based on zinc oxide nanowire arrays. *Science* (1979) 312, 242–246. <http://dx.doi.org/10.1126/science.1124005>.
- Wang, S., Xie, Y., Niu, S., Lin, L., Liu, C., Zhou, Y.S., Wang, Z.L., 2014. Maximum surface charge density for triboelectric nanogenerators achieved by ionized-air injection: Methodology and theoretical understanding. *Adv. Mater.* 26, 6720–6728. <http://dx.doi.org/10.1002/ADMA.201402491>.
- Xu, S., Qin, Y., Xu, C., Wei, Y., Yang, R., Wang, Z.L., 2010. Self-powered nanowire devices. *Nature Nanotechnology* 5, 366–373. <http://dx.doi.org/10.1038/nnano.2010.46>.
- Yang, J., Cao, J., Han, J., Xiong, Y., Luo, L., Dan, X., Yang, Y., Li, L., Sun, J., Sun, Q., 2022a. Stretchable multifunctional self-powered systems with Cu-EGaIn liquid metal electrodes. *Nano Energy* 101, 107582. <http://dx.doi.org/10.1016/J.NANOEN.2022.107582>.
- Yang, P., Wang, P., Diao, D., 2022b. Graphene nanosheets enhanced triboelectric output performances of PTFE films. *ACS Appl. Electron. Mater.* [http://dx.doi.org/10.1021/ACSAELM.2C00334/ASSET/IMAGES/LARGE/EL2C00334\\_0012.JPEG](http://dx.doi.org/10.1021/ACSAELM.2C00334/ASSET/IMAGES/LARGE/EL2C00334_0012.JPEG).
- Zhang, J., Hu, S., Shi, Z., Wang, Y., Lei, Y., Han, J., Xiong, Y., Sun, J., Zheng, L., Sun, Q., Yang, G., Wang, Z.L., 2021. Eco-friendly and recyclable all cellulose triboelectric nanogenerator and self-powered interactive interface. *Nano Energy* 89, 106354. <http://dx.doi.org/10.1016/J.NANOEN.2021.106354>.
- Zhang, R., Olin, H., 2020. Material choices for triboelectric nanogenerators: A critical review. *EcoMat.* 2, <http://dx.doi.org/10.1002/eom2.12062>.

- Zhang, Y., Zhou, Z., Sun, L., Liu, Z., Xia, X., Tao, T.H., 2018. Genetically engineered biofunctional triboelectric nanogenerators using recombinant spider silk. *Adv. Mater.* 30, 1–9. <http://dx.doi.org/10.1002/adma.201805722>.
- Zhao, L., Zheng, Q., Ouyang, H., Li, H., Yan, L., Shi, B., Li, Z., 2016. A size-unlimited surface microstructure modification method for achieving high performance triboelectric nanogenerator. *Nano Energy* 28, 172–178. <http://dx.doi.org/10.1016/j.nanoen.2016.08.024>.
- Zheng, Y., Liu, T., Wu, J., Xu, T., Wang, X., Han, X., Cui, H., Xu, X., Pan, C., Li, X., 2022. Energy conversion analysis of multilayered triboelectric nanogenerators for synergistic rain and solar energy harvesting. *Adv. Mater.* 34, 2202238. <http://dx.doi.org/10.1002/ADMA.202202238>.
- Zheng, Q., Shi, B., Li, Z., Wang, Z.L., 2017. Recent progress on piezoelectric and triboelectric energy harvesters in biomedical systems. *Adv. Sci.* 4, 1–23. <http://dx.doi.org/10.1002/advs.201700029>.
- Zhou, M., Al-Furjan, M.S.H., Zou, J., Liu, W., 2018. A review on heat and mechanical energy harvesting from human – Principles, prototypes and perspectives. *Renew. Sustain. Energy Rev.* 82, 3582–3609. <http://dx.doi.org/10.1016/j.rser.2017.10.102>.
- Zhu, J., Zhu, M., Shi, Q., Wen, F., Liu, L., Dong, B., Haroun, A., Yang, Y., Vachon, P., Guo, X., He, T., Lee, C., 2020. Progress in TENG technology—A journey from energy harvesting to nanoenergy and nanosystem. *EcoMat.* 2, 1–45. <http://dx.doi.org/10.1002/eom2.12058>.